MEASURING & MODELLING THE INSTRUMENTED INDENTATION (NANOINDENTATION) RESPONSE OF COATED SYSTEMS

T F Page, S J Bull

MEASURING & MODELLING THE INSTRUMENTED INDENTATION (NANOINDENTATION) RESPONSE OF COATED SYSTEMS

Journal:	*Philosophical Magazine & Philosophical Magazine Letters*
Manuscript ID:	TPHM-05-Dec-0569.R1
Journal Selection:	Philosophical Magazine
Date Submitted by the Author:	20-Feb-2006
Complete List of Authors:	Page, T; University of Newcastle Bull, S J; University of Newcastle, School of Chemical Engineering and Advanced Materials
Keywords:	tribology, coatings, hardness, nanoindentation
Keywords (user supplied):	Elastic Modulus, Scale-Effects

MEASURING & MODELLING THE INSTRUMENTED INDENTATION (NANOINDENTATION) RESPONSE OF COATED SYSTEMS

T.F. PAGE and S.J. BULL
Advanced Materials Group,
School of Chemical Engineering & Advanced Materials,
University of Newcastle,
Newcastle upon Tyne,
NE1 7RU,
UK.

Submitted to *Philosophical Magazine*

for the special issue on

Instrumented Indentation

(ECI Crete October 2005)

Communicating author

Professor Trevor page

Pro-Vice-Chancellor for External Affairs & Research Liaison
University of Newcastle upon Tyne
6 Kensington Tce
Newcastle upon Tyne
NE1 7RU

Phone - 0191 222 7701

Fax - 0191 222 8480

Email pvc-research@ncl.ac.uk

Word length 5494 (inc. abstract, keywords, refs & fig captions) + 7 figures

Original submission 22 Dec 2005

Revised 14 February 2006

FINAL REVISE for typos etc 05.04.06

MEASURING & MODELLING THE INSTRUMENTED INDENTATION (NANOINDENTATION) RESPONSE OF COATED SYSTEMS

T.F. PAGE and S.J. BULL
Advanced Materials Group,
School of Chemical Engineering & Advanced Materials,
University of Newcastle,
Newcastle upon Tyne, NE1 7RU, UK.

Abstract

We have been determining the ways in which *the mechanical properties of coated systems* – including those with very thin (<100nm) coatings - can best be characterised, at the appropriate small spatial scales, using instrumented indentation techniques (IIT). Our approaches have been to critically assess the differing types of sample information available from load-displacement (P-δ) curves, P-δ^2 analyses and P-S^2 data (where S is the contact stiffness). Parallel insights into the deformation mechanics controlling the contact response have been sought using transmission electron microscopy (TEM), high resolution scanning electron microscopy (HRSEM) and scanning probe microscopy (SPM) to characterise both the detailed appearance of resultant indentations and their underlying deformation structures.

Increasingly, many coatings are multilayered and thus there is a need for a modelling approach that can predict the mechanical properties of any proposed multilayer design. Since testing all possible stack sequences and combinations is impossible, we have successfully developed an energy-dissipated-per-unit-volume-of-plastic-zone model to predict the effective hardness, elastic modulus and IIT response in such cases.

Such studies are furthering our understanding of the fundamental origins of the mechanical behaviour of coated systems, with particular emphasis on the scale sensitivity of responses and with the purpose of informing systems' design. New insights have occurred such as the differing scale-sensitivities of system hardness (H_{sys}) and elastic modulus (E_{sys}) resulting in there being a critical range of contact scale range over which a maximised elastic contact response can be expected.

Key words: nanoindentation, coatings, tribology, scale-effects, hardness, elastic modulus.

1. Instrumented Indentation Testing IIT) - an ideal investigative tool at the length-scale of many coated systems

The use of individual thin (<1-10μm) coatings, and multi-layered coating sequences, is becoming increasingly widespread to effectively surface engineer the mechanical and physical properties of a range of engineering components [e.g. [1]]. While the beneficial effects of such coatings are usually out of all proportion to their thickness and volume fraction, their limited spatial thickness poses special challenges in both measuring, and understanding, the detailed mechanical responses of the coating-substrate system. This is especially critical at contact scales of the order of, or less than, the coating thickness (t) where the most significant property enhancements are usually experienced.

In such cases, instrumented indentation techniques (e.g. nanoindentation) are a particularly attractive investigative tool because:

a) at low loads, nanoindentation offers one of the few possibilities for experimentally determining *the properties and responses of the coating material itself in the microstructural and residual stress state in which it is being used* (e.g. [2-6]). Not only can this be useful as a diagnostic of processing quality and reproducibility, but many materials used for coatings (e.g. TiN and various hard carbon and carbon nitrides) do not otherwise exist in bulk form for property measurements;

b) the scale of many coatings is commensurate with that where *significant size- or length-scale effects* on properties are expected, thus negating the use of 'text book' or bulk property values in system design - even when such values are well-known (e.g. [7]);

c) by performing indentations as a function of load, *the system responses can be determined as a function of contact scale* and thus the varying contributions of the coating and the substrate quantitatively measured and modelled (e.g. [4-6, 8-10]); in turn, this can provide *a critical basis for the necessary understandings of property control necessary to underpin effective, fit-for-purpose, system design;*

d) Arrays of nanoindentations can be used to assess the *point-to-point variability and reliability of the system*, thus allowing the efficacy of both processing and production control to be monitored non-destructively. Such arrays are also invaluable to assist the location of indentations for microscopy (e.g. [11, 12]).

Though nanoindentation techniques are now well-established and widely-used, too much emphasis is perhaps still placed on simply measuring system properties (e.g. hardness and elastic modulus). By contrast, we have developed a range of approaches which allow considerable understandings to be gained of the *ways in which coated systems work as a function of contact scale*; these are

(1) the detailed appraisal of load-displacement (P-δ) curves (the "*system mechanical fingerprint*" (e.g. [2-6, 9-12]));
(2) detailed analyses of the load-displacement-squared (P-δ^2) response (e.g. [5, 13-14]);
(3) the novel use of load-verses-contact-stiffness-squared (P-S^2) data [15];
(4) the use of microstructural techniques to reveal the detailed deformation mechanisms responsible for the contact response, and

(5) predictive performance modelling of the behaviour of coatings, very thin coatings and multilayer stacks (e.g. [9, 16-19]).

The following examples demonstrate the power of these approaches.

2. Experimental

Four different NanoIndenter™ II and XP instruments (Nano Instruments Inc, Oak Ridge, TN) were used at the Materials Division, University of Newcastle (UK), the Microstructural and Micro analytical Sciences group (MMS) (Oak Ridge National Laboratory (ORNL)), the High Temperature Materials Laboratory (HTML) at ORNL and at Nano Instruments' demonstration laboratory, where the XP incorporated the latest-design 'Continuous Stiffness Module' (CSM) for continuously measuring *S*. Further a Hysitron Triboindenter™ was employed in Newcastle. All used standard Berkovich indenters and were calibrated to manufacturers' standard specifications (including frame compliance and tip radius).

Samples comprised a range of coated systems on both ideal (e.g. single crystal) and engineering materials substrates chosen to have different thicknesses of coating and systematic variations either in elastic modulus or hardness between coating and substrate.

Indentation load ranges were chosen to test as wide a range of indentation depths relative to the coating thickness (β) as possible. Typically, each experiment was repeated ten times and many were performed using the constant loading rate (*dP/P)* loading sequence of Lucas *et al.* [20] which enables large numbers of data points to be accumulated in the low-load end of each data set - something particularly useful when undertaking single experiments over wide load ranges (e.g. [15]). For example, compare the initial loading curve segments of figures 1(b) and 1(c) with figure 1(d) which used the dP/P method.

Data was analysed using standard Nano Instruments' and Hysitron' software to generate data streams for P, δ and S from which plots of P-δ, P-δ^2 and P-S^2 were created. Standard Nano Instruments' Software was also used with the data from the XP system to generate plots of sample hardness and Young's modulus as a function of indenter plastic displacement.

Indentation sites were examined by HRSEM using either a Camscan 40DV (LaB_6-sourced) SEM in Newcastle or a Philips XL30 field-emission-sourced instrument at ORNL.

3. The appraisal and analysis of *P-δ* curves

Detailed appraisal of P-δ curves from complete indentation loading and unloading cycles can yield both qualitative and quantitative insights into the responses of coated samples, as the following sections demonstrate.

3.1 Comparison of the P-δ curve (the P-δ "fingerprint") for a coated system with that of the substrate alone at the same maximum load.

This is the first critical step in revealing the changes in response caused by the coating. For example, figure 1(a) readily and simply reveals that applying ~5 μm of a TiN coating to an EN 24 steel has conferred a reduction in the maximum indenter displacement at a given contact load, reductions in the elastic and plastic works of indentation (that is, the areas bounded by the P-δ curves e.g. [2, 4, 21]), a lower residual displacement on unloading and a critical load value

(~450mN) at which the system reverts from coating-domination to substrate-control during loading [2-6]. Similarly, figures 1 (b) & (c) show *P-δ* plots for an EN 304 stainless steel substrate with and without ~1μm of hard amorphous carbon. By comparison of equivalent curves at the peak loads of 1, 5 & 10 mN peak loads, not only are the very large reductions in penetration, work of indentation and final elastically-recovered residual depth due to the coating again clearly revealed but in the inset 1*mN* plots, it is also clear that a w*holly elastic response* has been conferred on the system at displacements of up to ~30nm. For a particular application, this may be the most significant improvement looked for in using the coating. [22].

3.2 Detecting the presence of displacement discontinuities in loading curves ("pop-ins")

'Pop-ins' (discrete discontinuities) in *P-δ* curves witness either dislocation nucleation in the coating or the substrate (i.e. an elastic-plastic transition) [2, 11, 12] or the nucleation of stress-relieving through-thickness cracks in the coating (i.e. the onset of coating fracture) (e.g. [2-4]). Figure 1(d) shows the first such (arrowed) pop-in in a SiC-coated silicon sample (loading below this point resulting in a purely elastic response (c.f. figure 5(a)), while figure 2 reveals how microstructural characterisation or such crack paths can be important, not only in revealing the preferred, lowest-energy, microstructural or crystallographic crack paths in the coating but also, as here, often relating them to the behaviour of the underlying substrate (or vice versa). In this case, <110> cracking in the substrate is accommodated by orthogonal $<11\bar{2}0>$ and $<10\bar{1}0>$ crack segments in the coating, suggesting that the substrate cracked first. [23].

3.3 Using changes in characteristic P-δ discontinuities in the substrate as in-built 'stress-sensors'

For substrates displaying characteristic *P-δ* discontinuities from either dislocation generation (e.g. single crystal MgO [4]), cracking [2-4] or pressure-induced phase transformations (e.g. silicon) [e.g. 11,17], such materials' characteristic phenomena can be used as *'in-built' contact stress sensors to calibrate the extent to which load support is now borne by the coating* [4,23]. For example, figure 1(d) shows that the characteristic "reverse thrust" in the substrate-only curve due to the reverse densification transformation in silicon has completely disappeared from the coated system curve demonstrating that, at this contact scale and for this thickness of coating, densification of the substrate has been avoided by a quantifiable amount of load support (P_{sup} ~20mN) by the coating.

3.4 Determining the unloading contact stiffness

The slope of the upper portion of the unloading curve (which is related to the contact elastic modulus [24])) can usefully reveal whether the elastic recovery of the indentation depth on unloading is dominated by the coating (which, therefore, must still be sufficiently intact to be significantly load-supporting), or only the substrate. The almost exactly parallel slopes of the two unloading curves on figure 1(a) show that, in both cases, control is by the substrate alone showing that, at this peak load, the coating is sufficiently cracked to be offering little in terms of stresses driving elastic recovery. [4]).

3.5 Looking for fine detail, especially in the very low load portions of loading curves

This is discussed later in section 6 and figure 5.

4. The P-δ^2 analysis

Hainsworth *et al.* [13] showed that the loading curve of homogeneous samples could be well-described by a linear relationship, $P = K_m\delta^2$, between load and displacement squared. By superposing the expected elastic and plastic displacements beneath the indenter, the constant K_m was derived as having the form

$$K_m = E\left(\phi_m\sqrt{\frac{E}{H}} + \psi_m\sqrt{\frac{H}{E}}\right)^{-2} \quad (1)$$

where E and H respectively describe the Young's modulus and hardness of the sample. All properties for the diamond indenter, including its effect on the contact modulus, were absorbed into the constants ϕ_m *and* ψ_m which, for a Berkovich indenter, were found to have the values 0.194 and 0.930 respectively [13]. The values of these constants were also later derived by Malzenbender et al. [28] in terms of the indenter geometry constraints used by Oliver and Pharr [24]. However, further study is still needed here to properly allow for effects such as the load-bearing pile-up of displaced material around the indentation and any sensitivity to the geometrical factors used in the data analysis for E and H (e.g. in the Sneddon equation) (e.g. [29, 30]).

In a later paper, Hainsworth and Page [14] demonstrated that a similar approach can be used to analyse the performance of coated systems whereby the initial portion of the P-δ^2 plot is expected to be a straight line segment determined by the mechanical properties of the coating with this progressively changing, at increasing loads, to a second straight line segment-controlled by the properties of the substrate. This has been successfully used to provide *a tractable experimental approach to determining the range of loads and displacements over which the coating is found to dominate system behaviour and in which "coating only" properties can be measured* (thus removing the reliance on empirical rules such as working at displacements less than 10% *t*) [5-6, 17].

Figure 3 (a) demonstrates this approach for a-1μm coating of 3C-SiC on (100) silicon. While the Si substrate alone shows linear P-δ^2 behaviour over the whole load range, the coated system displays three different regimes; I - coating dominated response (up to ~5-10mN); II - coating and substrate jointly dominated region (10-100mN); III - substrate dominated response (>100mN) which is parallel to that for the Substrate only.

Based on such observations (e.g. [5, 8, 9]), figure 3(b) schematically represents a global picture of the measured hardness response of a coated system as a function of relative indentation depth, β. The example shown is for a hard coating on a softer substrate, with the regimes I-III corresponding to those identified from the P-δ^2 plot in figure 3(a). That the hardness of the system continues to show some enhancement beyond β = 1 is due to the constraining effect of the coating beyond the contact site on the flow of underlying material caused by substrate plasticity [10]. Such studies have led to sound models for the variation of system hardness and elastic modulus as a function of contact scale (e.g. [8, 9]).

In a further paper, McGurk and Page [6] showed that point-by-point differentiation of P-δ^2 plots can reveal additional fine details of the mechanical performance of coated samples, including crack nucleation events, which can further inform such property models.

5. The P-S^2 approach

Joslin and Oliver [31] were the first to suggest that the parameter P/S^2 was a materials characteristic which, like P/δ^2, was expected to be a constant for homogeneous samples. S, the stiffness of the sample-indenter contact can be measured either from the slope of the upper part of the unloading curve at a given load or by using a small superposed AC fluctuation in the loading current which allows the contact stiffness to be measured continuously along the loading curve [15, 31]. Attractively, P/S^2 should be largely independent of contact area and thus detailed indenter shape [31]. Like P/δ^2, this parameter is expected to show significant change as the contact response of a coated system changes from coating-domination to substrate control. Page et al. [15] were the first to explore the possible application of P/S^2 to coated systems and to perform a sensitivity analysis on variations in materials' H and E values to show that such changes in P/S^2 were potentially greater than those in P/δ^2 for the same system. However, experimentally, they discovered that, for hard-coated systems, the predicted changes in P/S^2 were accompanied by unexpectedly large maxima during the change from coating to substrate control.

The parameter P/S^2 is given by

$$\frac{P}{S^2} = \frac{\pi P}{4A\left(E^*\right)^2} = \frac{\pi H}{4\left(E^*\right)^2} \qquad (2)$$

where A is the contact area and thus reduces to a simple function ($\propto H/E^{*2}$) of the effective system hardness, H_{sys}, and the reduced contact elastic modulus, E^* ($=E_{sys}$) (e.g. [32]). The simpler parameter H/E is often used as a measure of the dominance of either elastic or plastic responses to contact stresses in tribological systems and is related to the plasticity index of Greenwood and Williamson [33] with increasing H/E values implying a shift to more elastically-dominated contact responses. The parameter H/E^2 should be an even more sensitive measure.

Figure 4 shows the variation in H_{sys}, E_{sys} and P/S^2 for a system comprising 2.3μm of TiN on a hard ASP23 tool steel. As with other homogeneous solids, P/S^2 is a constant for the substrate alone [15] but, for the coated system, a large broad maximum is observed extending to ~$t/5$. This strongly suggests that elastic behaviour could dominate asperity contacts well beyond the individual maxima in either H_{sys} or E_{sys} alone. The reason for this is that E_{sys} decreases faster with contact depth than does H_{sys} (e.g. [34, 35]) and thus this significant maximum in P/S^2 only emerges when the two parameters are considered together rather than separately [15].

6. Thinner coatings: sharper tips and lower loads

An important practical problem in measuring 'coating only' hardness values in systems with either very thin coatings, very hard coatings, soft substrates, or combinations thereof, is to ensure that, at suitably small indenter displacements, it is *only the coating and not the substrate which is plastically deforming* (e.g. [2]). In mechanics terms, the necessary requirement is that the maximum in the contact shear stress (which is at a small, contact-size-related, depth below the surface [e.g.32]) should not only lie in the coating but also exceed its shear yield stress before the longer-range components of this same stress can cause plastic yield in the substrate [e.g. 2, 6, 36]. In such cases, simple estimates of the shear stresses in both the coating and the substrate can be estimated from Hertz mechanics and provide an invaluable aid to experimental planning and interpretation (e.g. [36]). Thus, generally, thinner coatings require lower loads, coupled with smaller radius indenters, to fulfil these criteria. Even then, there may still be significant substrate influence on the indentation

response and quantitative modelling may still be required to extract reasonable 'coating only' values for H and E (e.g. [8,16-19]).

Figure 5(a) shows the effect of increasing tip sharpness in moving from an 'elastic-only' coating contact response to an elastic-plastic one; while figure 5(b) demonstrates the types of information which can be revealed by careful observation and analysis of the very low load portions of P-δ curves with a sharp tip where quantifiable effects include the transition from roughness dominated ($P \propto \delta$) to elastic ($P \propto \delta^{1.5}$) and then elastic-plastic deformation ($P \propto \delta^{2}$) on the variation of load with displacement [26, 27, 37]. A linear P-δ response can also result from the indenter simply flexing a "plate" of coating either debonded from the sample or traversing a void in the surface. Essentially, moving to sharper tips and lower loads can be thought of as moving the detailed responses seen in the very low load responses of materials (e.g. the effects of roughness and soft surface layers) to smaller displacements, though equivalent contact stresses [26].

Using a Hysitron Triboindenter with a ~50nm tip and operating at loads of <100μN with samples of coated and uncoated float glass, figure 6 shows that, although the resultant displacements are typically less than 20nm, there is clear evidence of plasticity occurring at all the indentations (c.f. figure 5(a)) with the differing mechanical responses of the two surfaces of the float glass clearly distinguished. For this material the 'upper' surface has been exposed to air during manufacture, while the 'lower' one has been in contact with liquid tin which is believed to diffuse into the glass with a maximum range of ~1μm (depending on process conditions) but to significantly increase both its hardness and elastic modulus over depths of less than a few hundred nanometres. Work is in progress to further clarify the dimensions of the Sn-affected material here. In terms of very thin coatings on this glass, figure 6(b) also shows the establishment of indentation plasticity (i.e. non-coincident P-δ loading and unloading curves) in experimental coatings of <200nm thicknesses at the required very small contact loads and scales.

7. Quantitative modelling – the energy dissipated per unit volume approach

Many coatings, especially for functional applications, are often multilayered with very thin (10-100nm) component layers. For successful applications, lifetime-critical mechanical behaviour, such as contact damage, need to be simultaneously optimised with the required functional response (e.g. tailored optical transmission). Since testing all possible stack sequences and combinations is impractical, we have developed a new energy-dissipated-per-unit-volume-based model for the composite hardness (as a function of contact depth) of multilayered systems [16-19].

Essentially the model sweeps an imagined plastic zone of increasing size (and containing all the deformation around the indentation volume [37]) through a particular stack sequence (such as that shown schematically in figure 7(a)) and, at any point, calculates the expected values of H_{sys} and E_{sys} given by

$$H_{sys} = \frac{\sum V_n H_0(n) + \sum A_n \gamma(n)}{V_p} \qquad (3)$$

and

$$E_{sys} = \frac{\sum V_n E(n)}{V_e} \qquad (4)$$

where the parameters *H(o), V* and *A* are the scale-independent hardness, volume and interfacial area of the n^{th} layer in the stack, V_p and $V_{e\ are}$ the volumes of the plastic and elastic zones and the γ-terms are correction factors to allow for additional size effects and constraints such as the differing plastic zone sizes in each layer etc (demonstrated schematically in figure 7(b)). Experimentally, good fits are found with $V_e \sim 8V_p$ [16-19], while the TEM and SEM micrographs shown as figure 1 in [37] clearly reveal that the plastic zone extends well beyond the indentation volume even in a material as hard as SiC.

For multilayer systems involving sequences of very thin layers, it is often impossible to obtain the individual components of the stack in sufficient thicknesses to make unambiguous component property measurements free of substrate influence. In such cases, models for the variation of systems hardness and modulus with scale are used to extract coating hardness and modulus values from experimental data for whatever suitable single layer systems may be available [8, 16-19].

Thus far, for very thin (<300nm) coatings consisting of single layers, bi-layers and multilayer stacks, good fits to real experimental data have been observed (e.g. [16-19]). However, for some multilayer stacks, a progressively poor fit suggests that, besides plastic deformation, contact-induced fracture may also be occurring. This prediction is borne out by sensitive in-situ acoustic emission (AE) evidence gathered during IIT experiments even when no cracks are visible in high resolution AFM and HRSEM images (e.g.[17-18]). This can be incorporated into the modelling [18-19] and an example is shown in figure 7(c). Here best-fit γ– values for the surface (γ_0) and for the interfaces between the different layers of the coating ((γ_1 - γ_5) were iteratively derived to be 0.5J/m^2 and the energy value for the interface between bottom layer of the coating and substrate was γ_6=100J/m^2. The initial simple model (upper solid curve) did not give a good fit to the experimental data inferring that through-thickness radial cracks may be occurring in one or more of the layers as confirmed by the AE. Thus the lower solid curve, which allows for through-thickness fracture of one of the layers, shows significantly improved agreement with the experimental IIT data at increasing loads [16-19].

8. Conclusions

This paper has demonstrated that IIT techniques are capable of providing far more information and insight into the behaviour of coated systems than simply only enabling calculation of H_{sys} and E_{sys}. In many cases, the insights into system performance, especially as a function of contacts scale, transcend any simple knowledge of mechanical property values. Our important conclusions are as follows:

(1) *P-δ* plots not only enable the property values and energetics of the system deformation to be determined as a function of scale but also often exhibit copious fine detail which witnesses either coating cracking, dislocation generation, the domination of surface roughness, elastic behaviour, soft surface layers and/or changes from coating to substrate domination etc.

(2) *P-* δ^2 analyses allow the scales at which (a) the coating dominates the system, (b) the substrate dominates the system and (c) the intermediate stage where both coating and substrate are both playing major, but changing, roles. The determination of K_m can also allow the calculation of both H_{sys} and E_{sys} values to be undertaken if one or the other is

already known and this can provide a valuable correlation with values obtained from P-δ data.

(3) P-S^2 analyses clearly show how the detailed system behaviour depends on the correlation of two parameters (in this case H_{sys} and E_{sys}) and reveals an unexpectedly broad contact depth regime in which elastic domination of surface tribological deformation is conferred by the coating. This regime is more significant than changes in either H_{sys} or E_{sys} alone would suggest.

(4) Information from very thin coatings can be obtained at low loads but only when the indenter is sharp enough to generate contact shear stresses large enough to produce full plasticity in the coating before the substrate yields. In other cases, elastic-only deformation may occur which allows values of the Young's modulus to be derived, through standard Hertz analysis, for correlation with those from P-δ and P-δ^2 analyses.

(5) For multi-layer coatings, modelling the system performance needs to be undertaken as an aid to interpreting the observed IIT behaviour. Good results have so far been obtained using an energy-based "law of mixtures" model.

There is a wealth of further insights into the behaviour of coated systems obtainable by IIT - e.g. investigating through thickness and interfacial fracture behaviour, measuring toughness values[5] and identifying creep and rate-sensitive behaviour [e.g. 38]. Many of these have recently been reviewed [38].

9. Acknowledgements

Work at Newcastle has been supported by EPSRC, EU TMR and Pilkington Technology Centre, Ormskirk, UK. TFP thanks the University of Tennessee (Knoxville (UTK)) for a Visiting Research Professorship during the summer of 1997 when the P/S^2 work was initiated and, similarly, Oak Ridge National Laboratory (ORNL) for making facilities and support available as a Guest Scientist for the same period. EPSRC (UK) is thanked for the provision and support for the Newcastle Nano Indenter and AFM facilities. Eric Herbert took part in this study as part of his first and higher degree programs in the Faculty of Engineering at UTK. Dr. Sarah Hainsworth, Dr Martin McGurk and Dr Eva Berastegui and Dr Isobel Arce-Garcia are thanked for useful discussions and the citation of their work. Dr Natalia Tymiak (University of Minnesota) is thanked for obtaining the data in figure 6 during a student exchange with Newcastle. Lynne Toase provided valued help with preparation of the manuscript.

10. References

(*Note: for brevity, the reader is also guided to the many references to the related work of others contained in the references cited below*).

[1] D. S. Rickerby and S. J. Bull, Surf. Coat. Tech., **39**/**40**, 1989, 315-328.
[2] T. F. Page and S. V. Hainsworth, Surf. Coat. Tech. **61**, 1993, 201-208.
[3] T. F. Page in *Solid-Solid Interactions*, 1996, (Eds M. J. Adams, B. J. Briscoe and S. K. Biswas)
(Imperial College Press and World Scientific Pub. Co. UK & USA), pp93-116.
[4] S. V. Hainsworth and T. F. Page, Journal of Non-Destructive Evaluation **17** (4-5), 2001, 275-298.
[5] S. V. Hainsworth, M. R. McGurk and T. F. Page, Surf. Coat. Tech., **102**, 1998, 97-107
[6] M. R. McGurk and T. F. Page, Journal of Materials Research, **14** (6), 1999, 2283-2295
[7] S. J. Bull, T. F. Page and E. H. Yoffe, Philosophical Magazine Letters, **59**, 1989, 281-288.

[8] A. M. Korsunsky, M. R. McGurk, S. J. Bull and T. F. Page, Surf. Coat. Tech., **99**, 1998, 171-183.

[9] M. R. McGurk, H. W. Chandler, P. C. Twigg and T. F. Page, Surf. Coat. Tech., **68/69,** 1994, 576 - 581; ibid **92**, 1997, 87-95

[10] S. V. Hainsworth, T. Bartlett and T. F. Page, Thin Solid Films, **236**, 1993, 214-218.

[11] T. F. Page, W. C. Oliver and C. J. McHargue, J. Mater. Res., **7,** 1992, 450-473

[12] T. F. Page, L. Riester and S. V. Hainsworth, Symp. Proc. Mats. Res. Society, **522**, 1998, 113-118.

[13] S. V. Hainsworth, H. W. Chandler, and T. F. Page, J. Mater. Res., **11**, 1995, 1987 - 1995.

[14] S. V. Hainsworth and T. F. Page, Symp. Proc. Mats. Res. Society, **436**, 1997, 171-176.

[15] T. F. Page, G. M. Pharr, J. C. Hay, W. C. Oliver, B. N. Lucas, E. Herbert, and L. Riester, Symp. Proc. Mats. Res. Society, **522**, 1998, 53-64.

[16] S. J. Bull, Mat. Res. Symp. Proc., **750**, 2003, 489-500.

[17] E. G. Berasategui, S.J. Bull and T. F. Page, Thin Solid Films **447-448**, 2004, 26-32

[18] S. J. Bull, E.G. Berasetegui and T. F. Page, Wear, **256,** 2004, 857-866.

[19] S. J. Bull, I. Arce-Garcia, E. G-Berasetegui and T. F. Page, Proc. 8th International Conference on Fracture Mechanics of Ceramics, Houston, February 25th-1st March 2003, *Active Materials, Nanoscale Materials, Composites, Glass and Fundamentals* **14,** (Eds. R.C. Bradt, D. Munz, M. Sakai and K.W. White), Springer, New York, (2005), pp 21-41.

[20] B. Lucas, W. C. Oliver, G. M. Pharr, and J. L. Loubet, Symp. Proc.Mats. Res. Society, **436**, 1997, 233 - 238.

[21] Y. T. Cheng and C. M. Cheng, Appl. Phys. Letts., **73**, 1998, 614 -616.

[22] T. Wright and T. F. Page, Surface and Coatings Technology, **54/55**, 1992, 557-562.

[23] E.G. Berasategui and T.F. Page, Surface & Coatings Technology **163-164,** 2003, 491-498

[24] W. C. Oliver and G. M. Pharr, J. Mater. Res., **7,** 1992, 1564 - 1583.

[25] S.V. Hainsworth and T. F. Page, Journal of Materials Science, **29**, 1994, 5529-5540.

[26] E. Gutierrez-Berasategui, *Determining the Properties of Thin-coated systems by Nanoindentation.* PhD Thesis, University of Newcastle upon Tyne, UK, 2003.

[27] I. Arce-Garcia, *Mechanical Properties of Fullerene-Like* CN_x PhD Thesis, University of Newcastle upon Tyne, UK, 2002.

[28] Malzbender J, With Gd, Toonder Jd. Journal of Materials Research, **15,** 2000, 1209-1212

[29] J. L. Hay, W. C. Oliver, A. Bolshakov and G. M. Pharr, Symp. Proc. Mats. Res. Soc., **522**, 1998, 101-112.

[30] B. Taljat, T. Zacharia, and G. M. Pharr, Symp. Proc. Mats. Res. Society, **522**, 1998, 33-38.

[31] D. L. Joslin and W. C. Oliver, J. Mater. Res., **5,** 1990, 123 – 126

[32] K. L. Johnson, *Contact Mechanics*, 1985, (Cambridge University Press, UK)

[33] J. A. Greenwood and J. B. P. Williamson, Proc. Roy. Soc. London, **A295**, 1966, 300-330

[34] R. B. King Int. J. Solids Structures, **23**, 1987, 1657-1664

[35] D. S. Stone, M. F. Tambwe, H. Kung, and M Nastasi, Symp. Proc. Mats. Res. Soc., **522**, 1998, 257-262.

[36] S. V. Hainsworth, S. J. Bull and T. F. Page, Symp. Proc. Mats. Res. Society, **522**, 1998, 433-438

[37] T. F. Page & S. J. Bull, Thin Solid Films, 2005, **484,** 439-442.

[38] S. J. Bull, J. Phys. D: Applied Physics, **38,** 2005, R393-R413

FIGURE CAPTIONS – SEPARATE VERSIONS

Figure 1

(a) P-δ plots for an EN 24 steel substrate with and without ~5 μm of TiN clearly show the benefits conferred by the coating (see text).
(b) & (c), P-δ plots for an EN 304 stainless steel substrate with and without ~1μm of hard amorphous carbon. In the inset 1mN plots, a wholly elastic response has been conferred on the system at displacements of ≤ 30nm.
(d) P-δ curves for a coated system comprising ~1 μm of SiC on (111) silicon again clearly showing the benefits conferred by the coating. The small arrowed pop-in in the coated system curve at ~300nm displacement signals the first of the ring-like cracks appearing in the coating shown in figure 2.

Figure 2

(a) as figure 1(c) but showing a series of loading 'pop-in' phenomenon each corresponding to the generation of stress-relieving "ring-like", through-thickness, cracks in the coating shown in figure (b) (SEM micrograph, secondary electron image, 5kV).
(c) A high magnification view of a similar crack in a ~200nm coated sample (see text).

Figure 3

(a) P-δ^2 curves for ~1μm 3C SiC on Si (111) and for Si (111) alone revealing the changing dominance of coating and substrate to system contact response (see text).
(b) A schematic plot showing the composite system hardness (H_c) displayed by a hard-coated system as a function of relative intention depth (β) together with schematic deformation regimes illustrating how either the coating or substrate, or both, controls the response. In this case, H_f is the hardness of the coating film and H_s is that of the substrate [8] (see text).

Figure 4

The variation of (a) H_{sys} and (b) E_{sys} and (c) P/S^2 with plastic depth for a 2.3μm TiN coating on an ASP23 tool steel substrate (see text).

Figure 5

(a) Load-displacement response from a CN_x coating on silicon showing elastic behaviour with a blunt tip and elastic-plastic behaviour with a sharp tip.
(b) A schematic portion of the load-displacement (P-δ) curve showing the differing quantifiable relationships between P and δ often observed at low loads (see text) [26, 27, 37].

Figure 6

(a) The clearly different P-δ plots from opposite sides of a commercial "float glass" sample made at very low loads (i.e. <100μN) and small displacements (<20nm) with a sharp (50nm radius) Berkovich indenter using a Hysitron Triboindenter.
(b) As (a) but with a number of very thin (<200nm) experimental coatings (see text). (Coatings: C: 200A SiO2; D: 100-150nm SiO2; E: 150-200nm SiO2 on TiO2).

Figure 7

(a) A schematic of the simple way in which the (hemispherical) plastic zone volume of the energy-law-of-mixtures-model is apportioned between the various deforming coating layers and the interfaces in a multilayer stack (see text).
(b) The probable type of discontinuity in plastic zone sizes between layers of different materials which are allowed for by the γ-correction factors.
(c) Experimental and modelled hardness-depth plots for a multilayer coating comprised of 3nm TiO_xN_y, 40nm SnO_2, 10nm Ag, 5nm Zr, 10nm ZnO and 20nm TiO_xN_y on float glass. In this case the model incorporates the effects of fracture (experimentally witnessed by in-situ acoustic emission (AE)) in the layers.

CRETE PAPER

FIGURES & FIGURE CAPTIONS

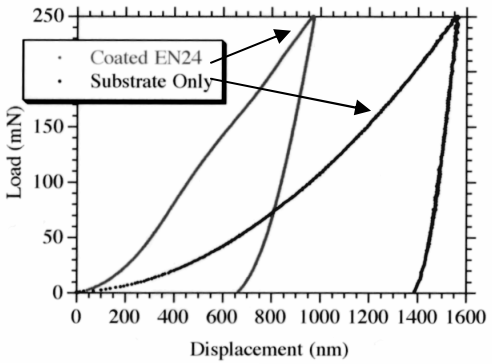

(a)

(b)

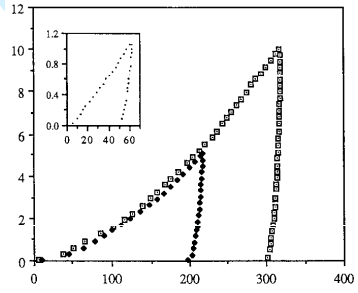

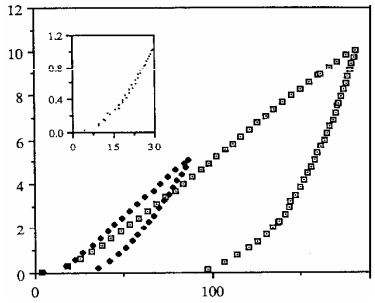

(c)

EN304 substrate **EN304 + 1µm hard carbon**

(d)

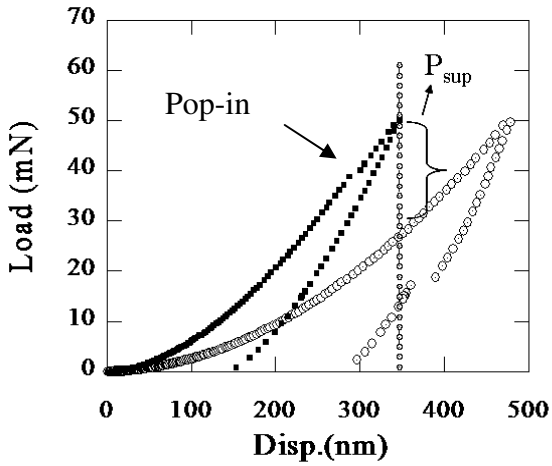

(100) Si +1µm SiC

Figure 1

(a) *P-δ* plots for an EN 24 steel substrate with and without ~5 µm of TiN clearly show the benefits conferred by the coating (see text).
(b) & (c), *P-δ* plots for an EN 304 stainless steel substrate with and without ~1µm of hard amorphous carbon. In the inset 1mN plots, a wholly elastic response has been conferred on the system at displacements of ≤ 30nm.
(d) *P-δ* curves for a coated system comprising ~1 µm of SiC on (111) silicon again clearly showing the benefits conferred by the coating. The small arrowed pop-in in the coated system curve at ~300nm displacement signals the first of the ring-like cracks appearing in the coating shown in figure 2.

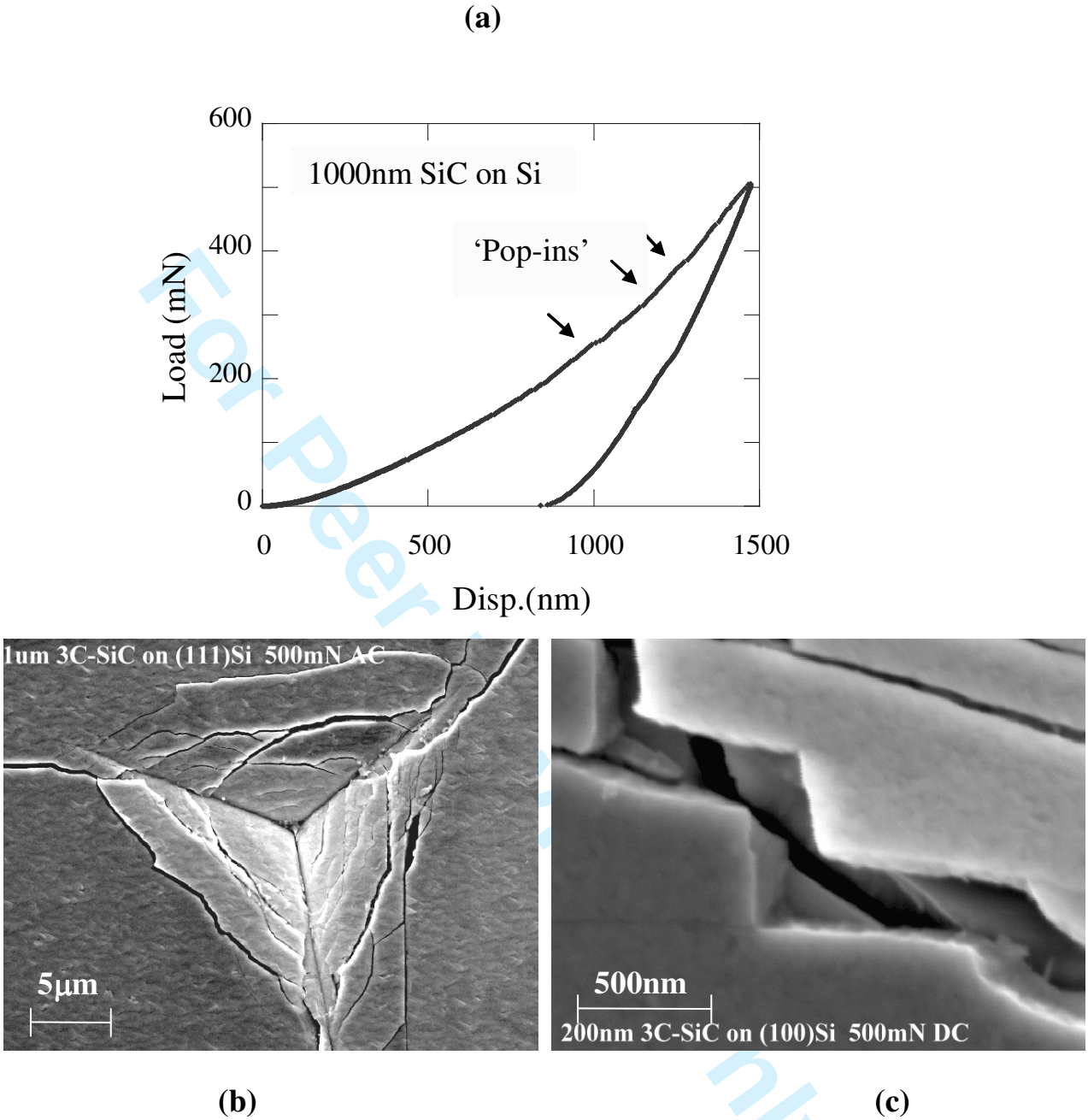

Figure 2.

(a) as figure 1(c) but showing a series of loading 'pop-in' phenomenon each corresponding to the generation of stress-relieving "ring-like", through-thickness, cracks in the coating shown in figure (b) (SEM micrograph, secondary electron image, 5kV).
(c) A high magnification view of a similar crack in a ~200nm coated sample (see text).

(a)

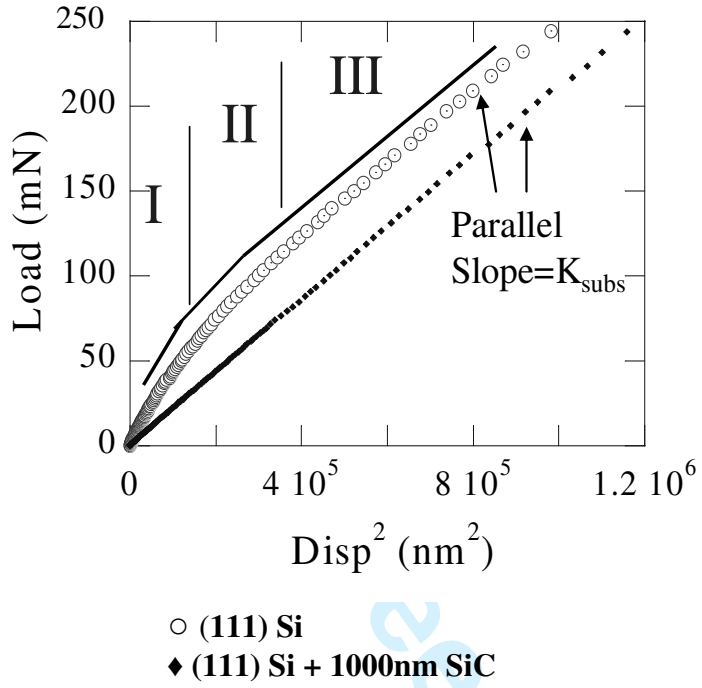

(b)

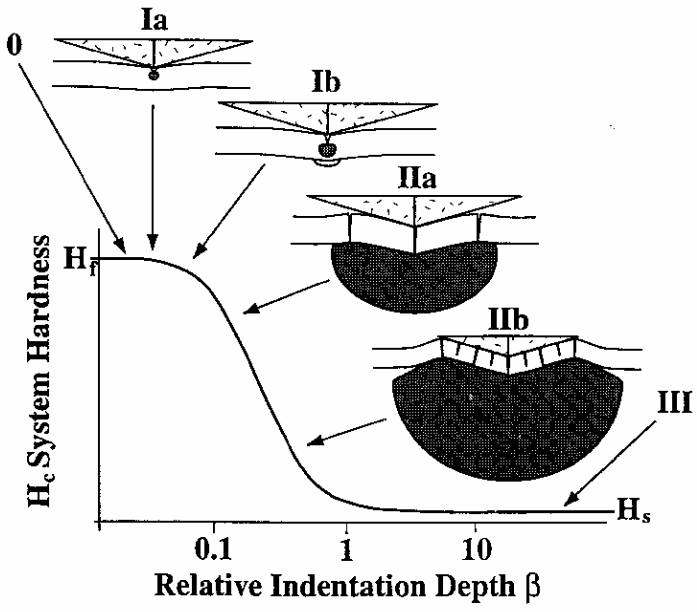

Figure 3

(a) $P\text{-}\delta^2$ curves for ~1μm 3C SiC on Si (111) and for Si (111) alone revealing the changing dominance of coating and substrate to system contact response (see text).
(b) A schematic plot showing the composite system hardness (H_c) displayed by a hard-coated system as a function of relative intention depth (β) together with schematic deformation regimes illustrating how either the coating or substrate, or both, controls the response. In this case, H_f is the hardness of the coating film and H_s is that of the substrate [8] (see text).

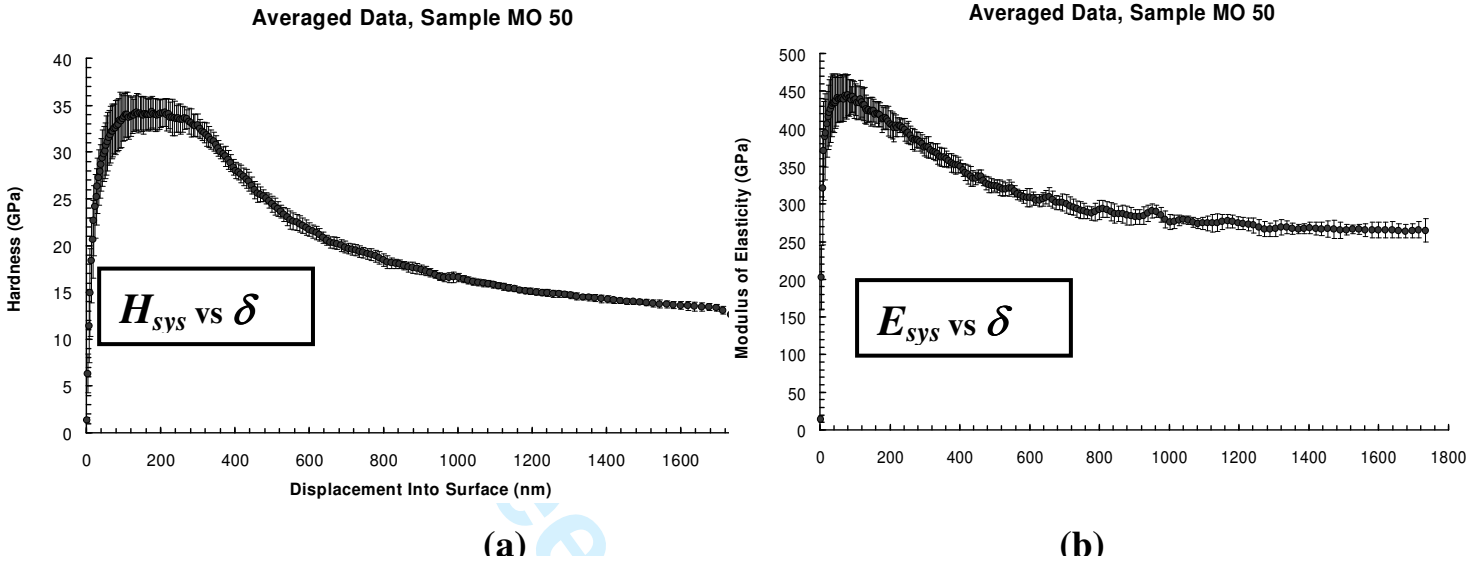

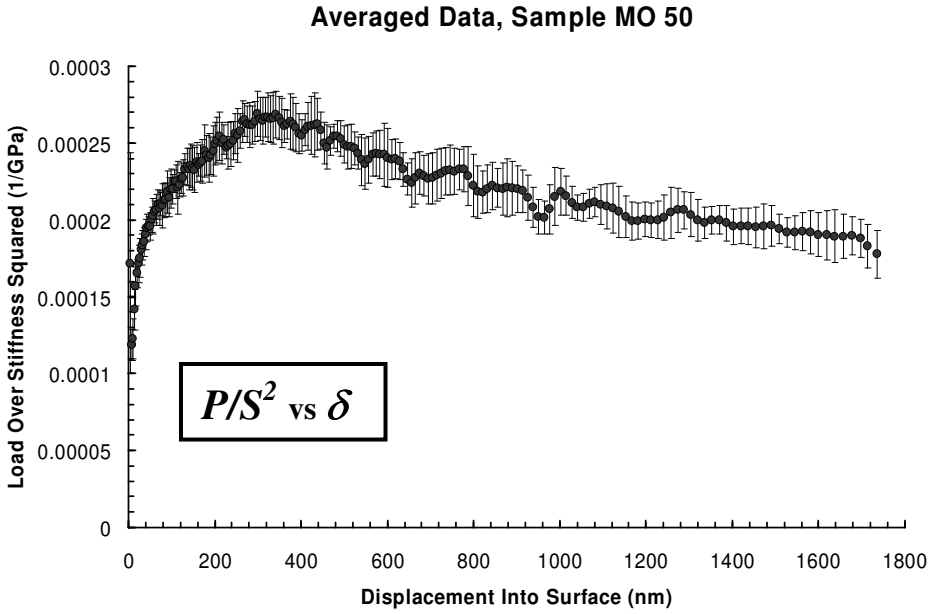

Figure 4

The variation of (a) H_{sys} and (b) E_{sys} and (c) P/S^2 with plastic depth for a 2.3μm TiN coating on an ASP23 tool steel substrate (see text).

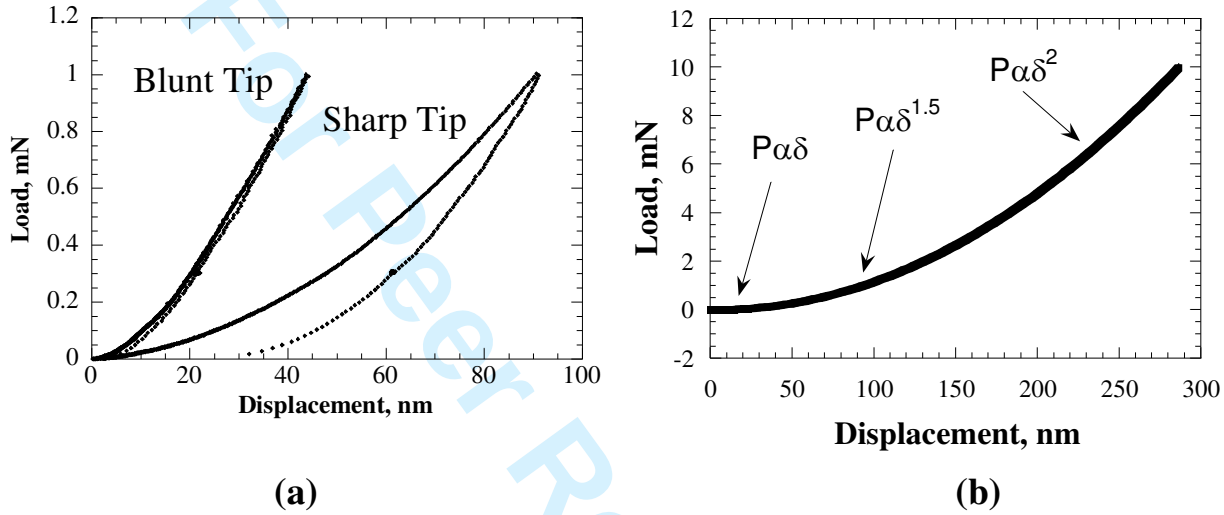

Figure 5:

(a) Load-displacement response from a CN_x coating on silicon showing elastic behaviour with a blunt tip and elastic-plastic behaviour with a sharp tip.
(b) A schematic portion of the load-displacement (P-δ) curve showing the differing quantifiable relationships between P and δ often observed at low loads (see text) [26, 27, 37].

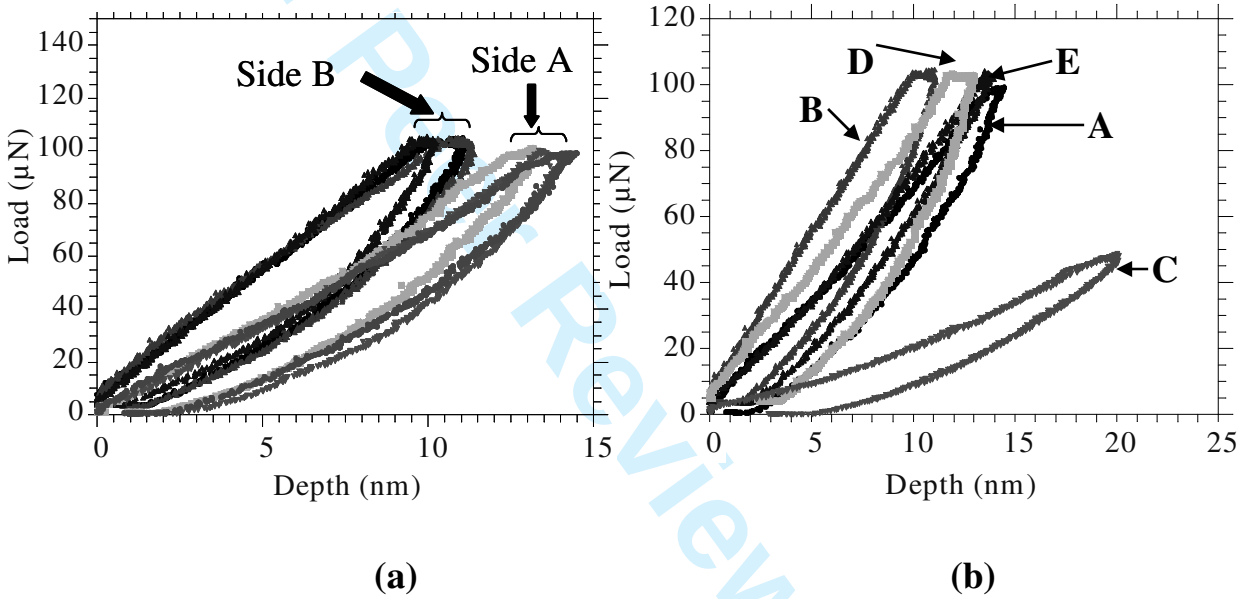

Figure 6

(a) The clearly different *P-δ* plots from opposite sides of a commercial "float glass" sample made at very low loads (i.e. <100μN) and small displacements (<20nm) with a sharp (50nm radius) Berkovich indenter using a Hysitron Triboindenter.

(b) As (a) but with a number of very thin (<200nm) experimental coatings (see text). (Coatings: C: 200A SiO2; D: 100-150nm SiO2; E: 150-200nm SiO2 on TiO2).

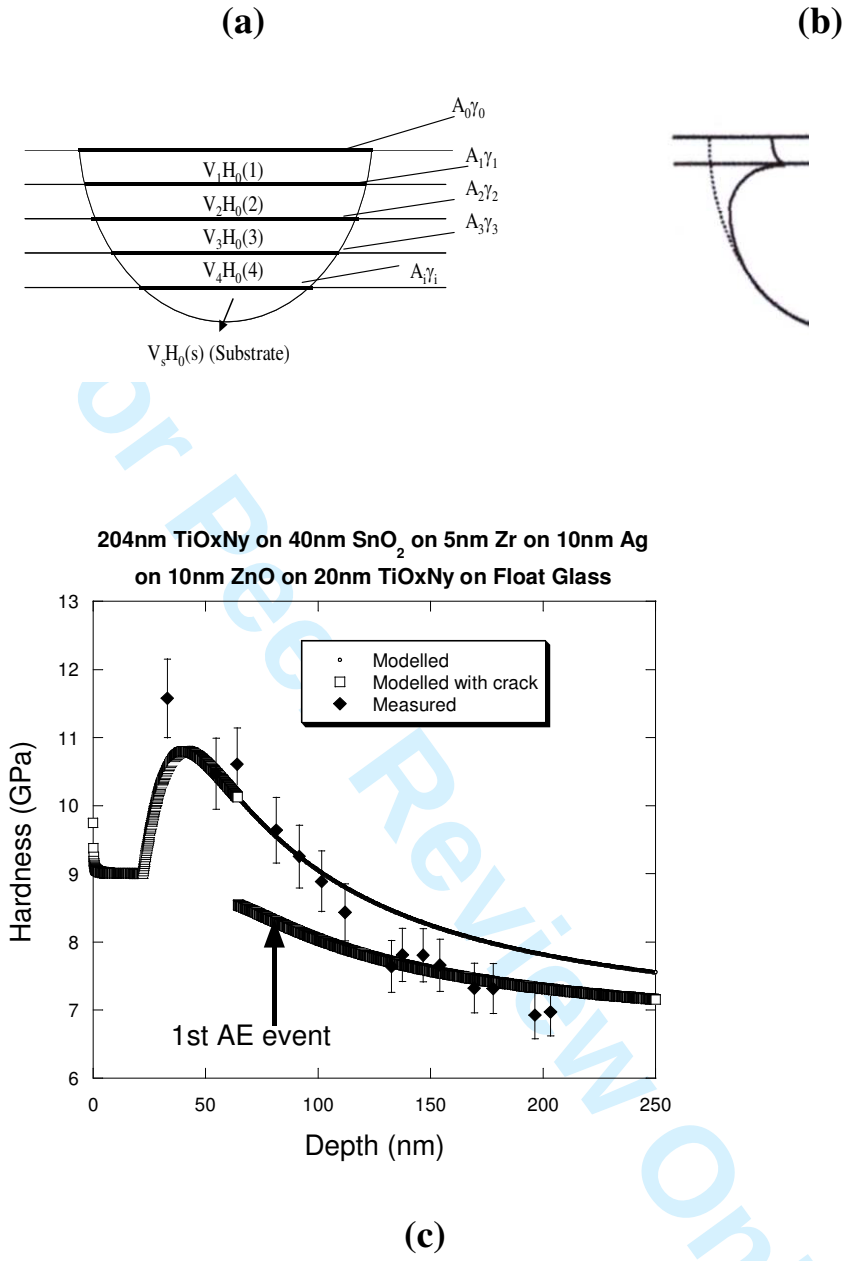

Figure 7

(a) A schematic of the simple way in which the (hemispherical) plastic zone volume of the energy-law-of-mixtures-model is apportioned between the various deforming coating layers and the interfaces in a multilayer stack (see text).
(b) The probable type of discontinuity in plastic zone sizes between layers of different materials which are allowed for by the γ-correction factors.
(c) Experimental and modelled hardness-depth plots for a multilayer coating comprised of 3nm TiO_xN_y, 40nm SnO_2, 10nm Ag, 5nm Zr, 10nm ZnO and 20nm TiO_xN_y on float glass. In this case the model incorporates the effects of fracture (experimentally witnessed by in-situ acoustic emission (AE)) in the layers.

PAGE & BULL - Phil Mag Paper

FIGURES & FIGURE CAPTIONS

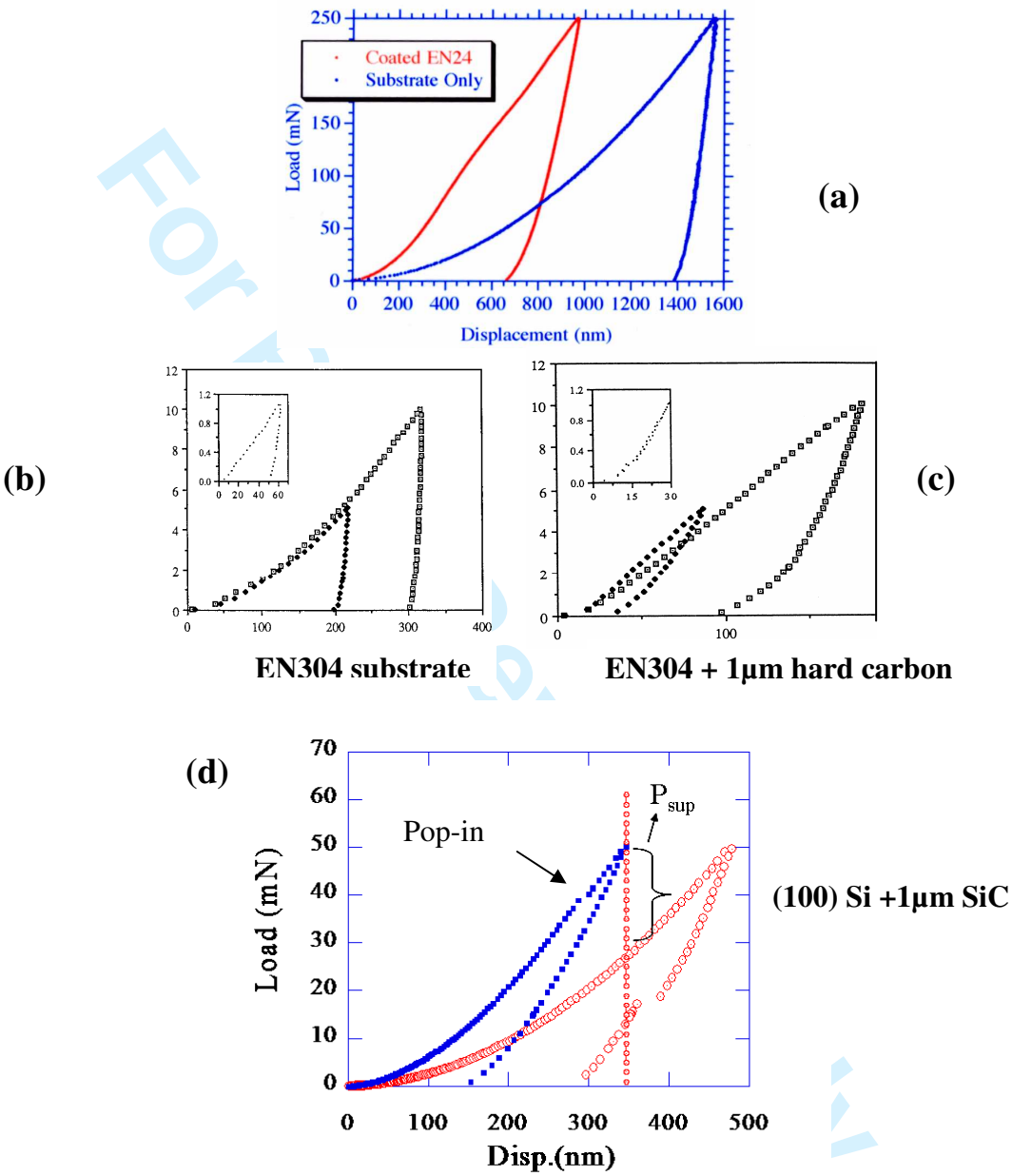

Figure 1

(a) *P-δ* plots for an EN 24 steel substrate with and without ~5 µm of TiN clearly show the benefits conferred by the coating (see text).
(b) & (c), *P-δ* plots for an EN 304 stainless steel substrate with and without ~1µm of hard amorphous carbon. In the inset 1mN plots, a wholly elastic response has been conferred on the system at displacements of ≤ 30nm.
(d) *P-δ* curves for a coated system comprising ~1 µm of SiC on (111) silicon again clearly showing the benefits conferred by the coating. The small arrowed pop-in in the coated system curve at ~300nm displacement signals the first of the ring-like cracks appearing in the coating shown in figure 2.

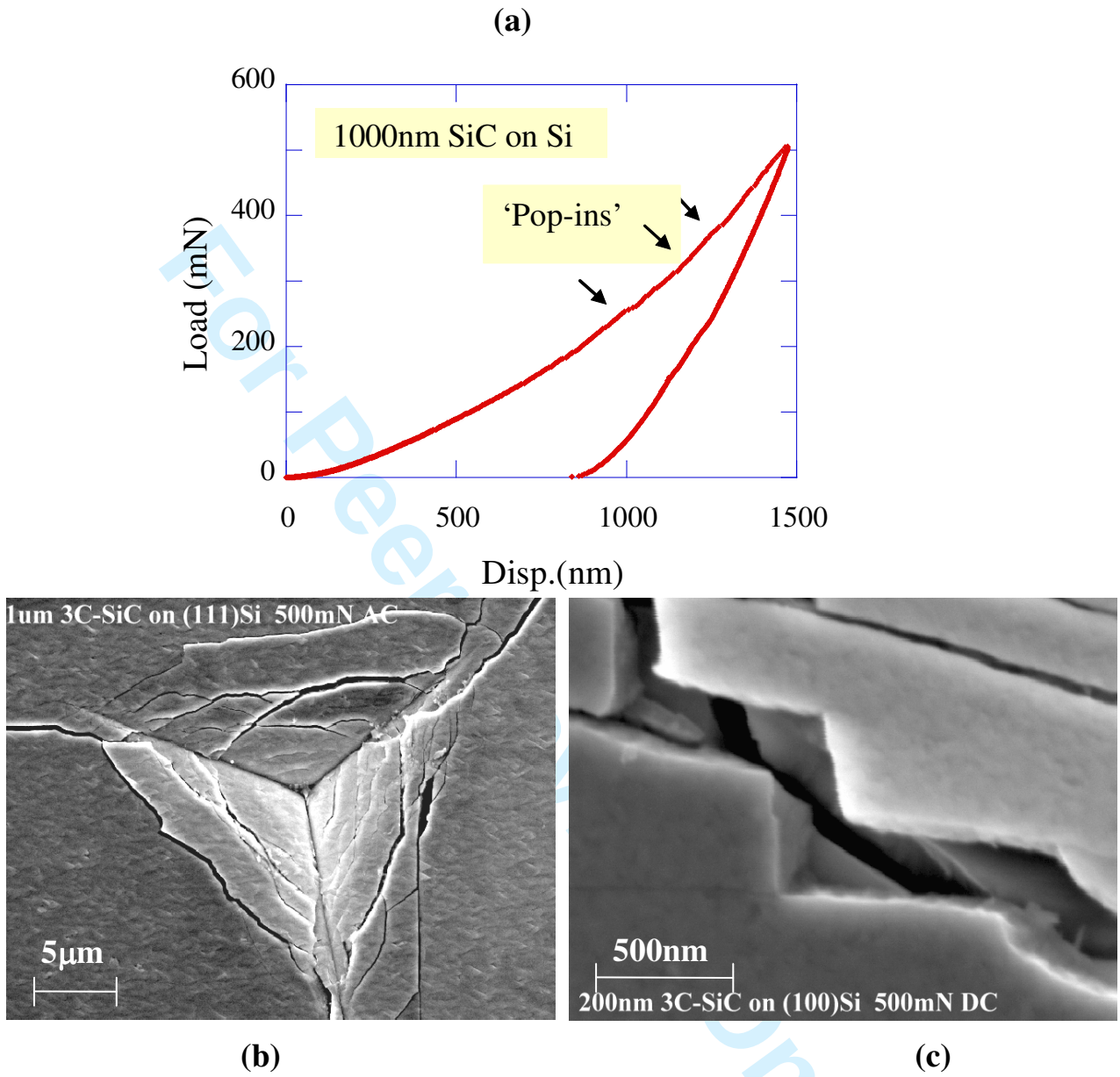

Figure 2.

(a) as figure 1(c) but showing a series of loading 'pop-in' phenomenon each corresponding to the generation of stress-relieving "ring-like", through-thickness, cracks in the coating shown in figure (b) (SEM micrograph, secondary electron image, 5kV).
(c) A high magnification view of a similar crack in a ~200nm coated sample (see text).

(a)

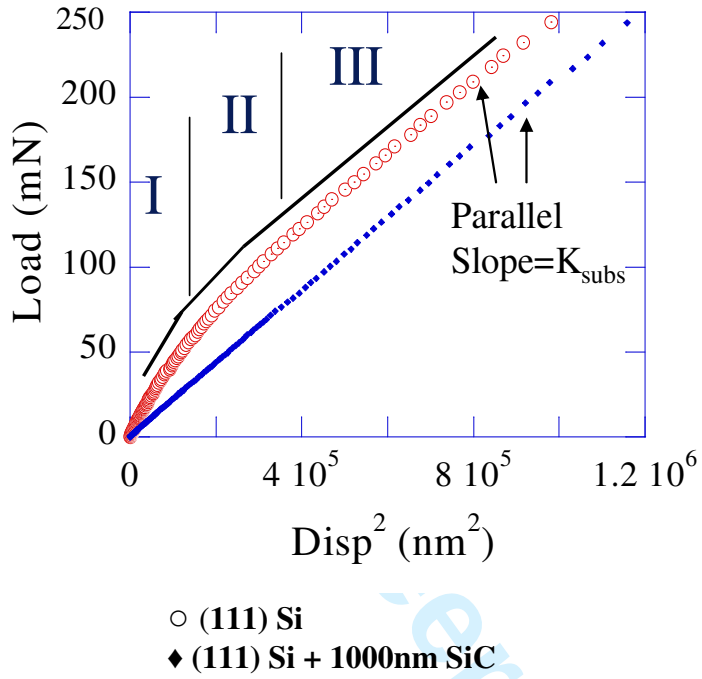

○ **(111) Si**
♦ **(111) Si + 1000nm SiC**

(b)

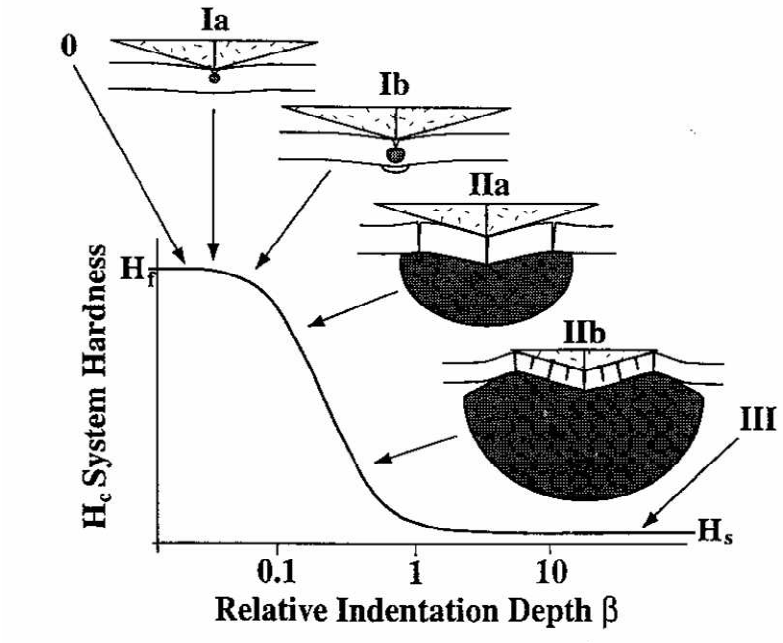

Figure 3

(a) $P\text{-}\delta^2$ curves for ~1μm 3C SiC on Si (111) and for Si (111) alone revealing the changing dominance of coating and substrate to system contact response (see text).
(b) A schematic plot showing the composite system hardness (H_c) displayed by a hard-coated system as a function of relative intention depth (β) together with schematic deformation regimes illustrating how either the coating or substrate, or both, controls the response. In this case, H_f i the hardness of the coating film and H_s is that of the substrate [8] (see text).

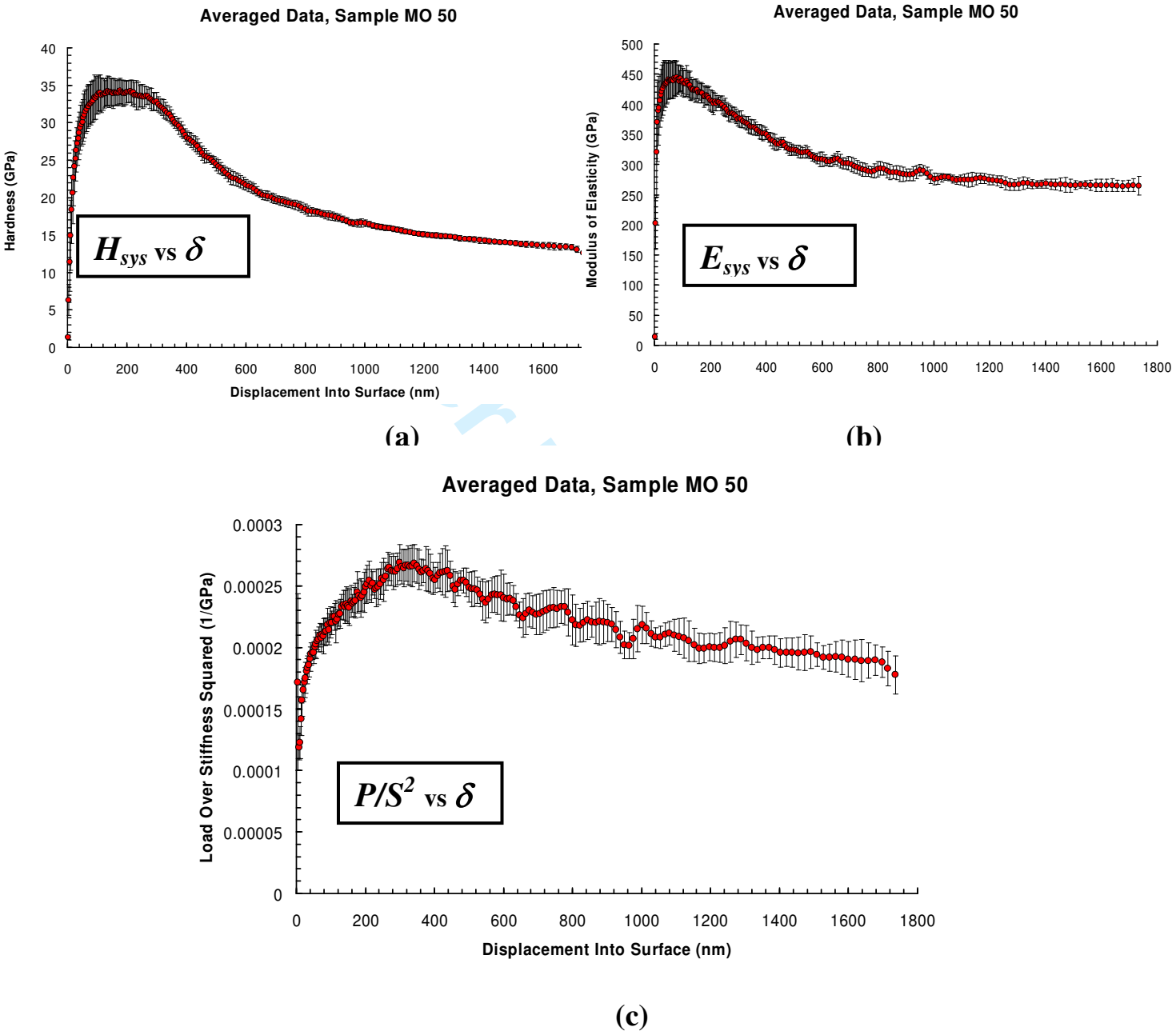

Figure 4

The variation of (a) H_{sys} and (b) E_{sys} and (c) P/S^2 with plastic depth for a 2.3μm TiN coating on an ASP23 tool steel substrate (see text).

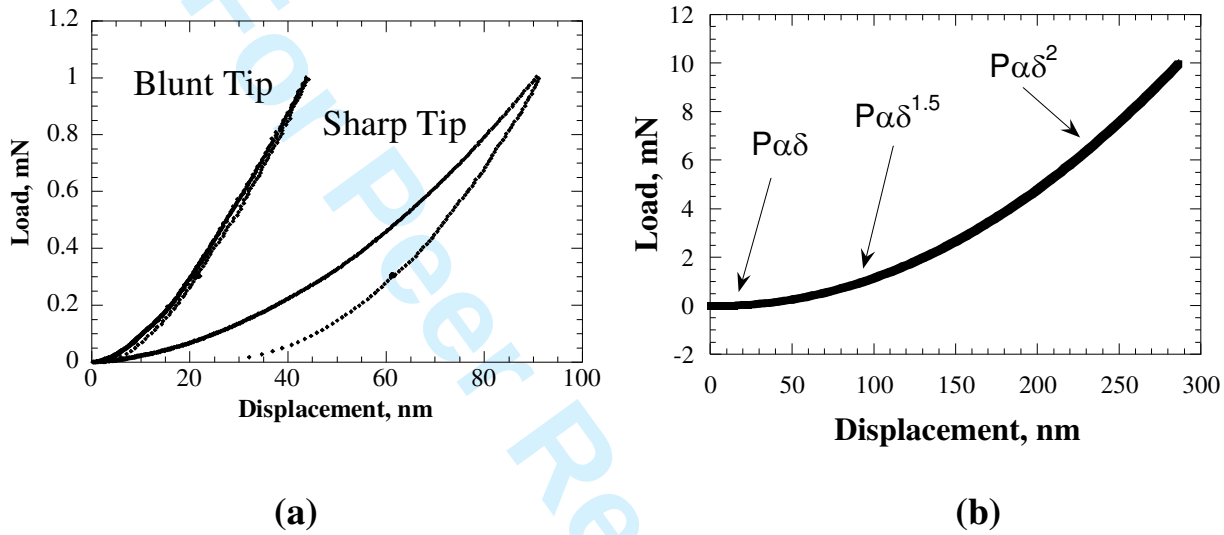

Figure 5:

(a) Load-displacement response from a CN_x coating on silicon showing elastic behaviour with a blunt tip and elastic-plastic behaviour with a sharp tip.
(b) A schematic portion of the load-displacement (P-δ) curve showing the differing quantifiable relationships between P and δ often observed at low loads (see text) [26, 27, 37].

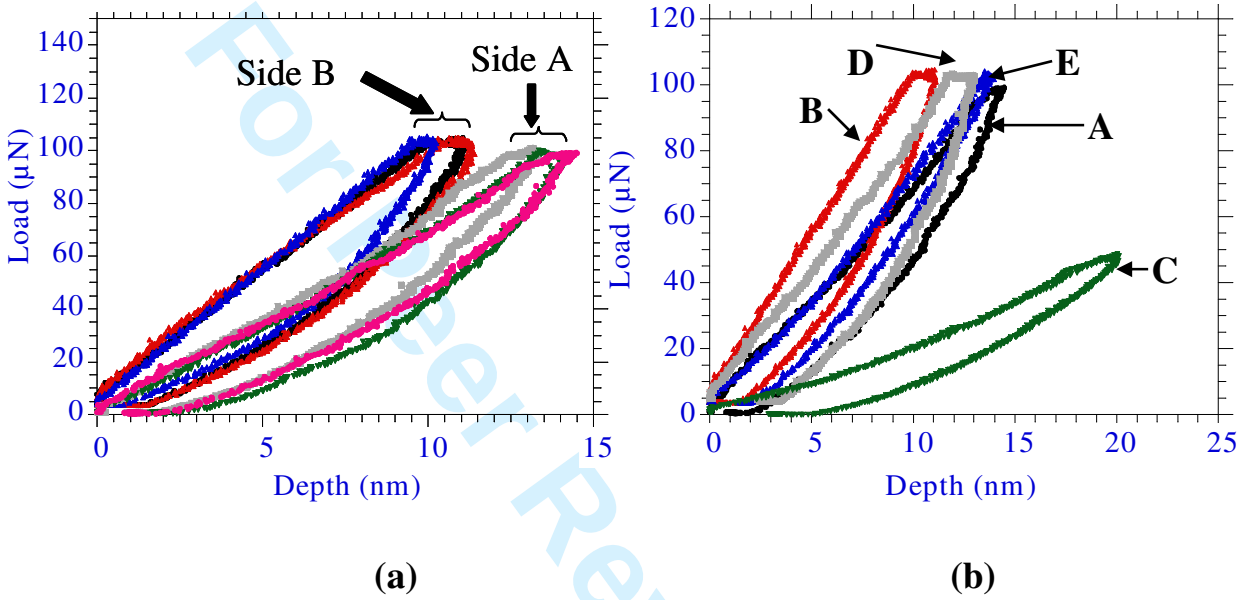

Figure 6

(a) The clearly different *P-δ* plots from opposite sides of a commercial "float glass" sample made at very low loads (i.e. <100μN) and small displacements (<20nm) with a sharp (50nm radius) Berkovich indenter using a Hysitron Triboindenter.

(b) As (a) but with a number of very thin (<200nm) experimental coatings (see text). (Coatings: C: 200A SiO2; D: 100-150nm SiO2; E: 150-200nm SiO2 on TiO2).

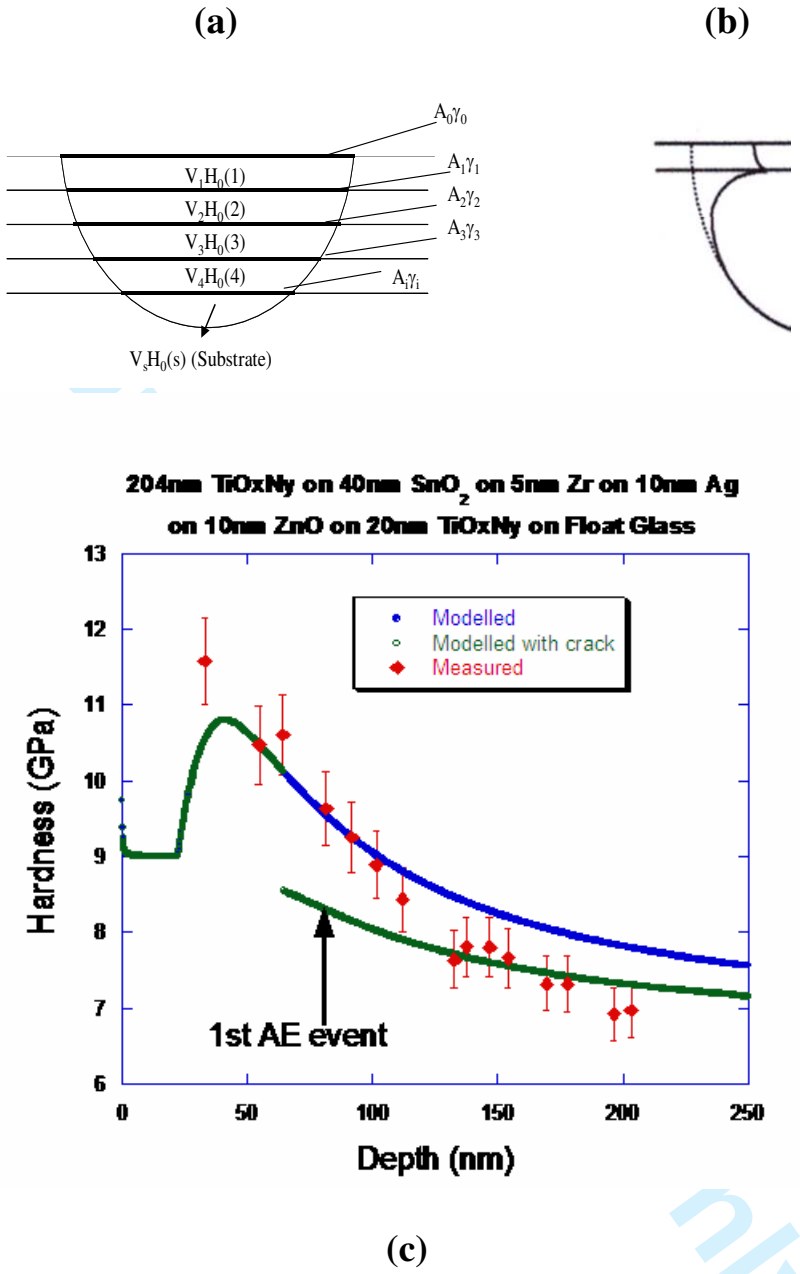

Figure 7

(a) A schematic of the simple way in which the (hemispherical) plastic zone volume of the energy-law-of-mixtures-model is apportioned between the various deforming coating layers and the interfaces in a multilayer stack (see text).
(b) The probable type of discontinuity in plastic zone sizes between layers of different materials which are allowed for by the γ-correction factors.
(c) Experimental and modelled hardness-depth plots for a multilayer coating comprised of 3nm TiO_xN_y, 40nm SnO_2, 10nm Ag, 5nm Zr, 10nm ZnO and 20nm TiO_xN_y on float glass. In this case the model incorporates the effects of fracture (experimentally witnessed by in-situ acoustic emission (AE)) in the layers.